Transactions of the Materials Research Society of Japan 24 [1] 1-5 (1999)

Defect Structure in Non-stoichiometric Epitaxially Grown $BaTiO_3$ Thin Film

Masayuki Fujimoto and Toshimasa Suzuki
Taiyo Yuden Co., Ltd.
5607-2 Nakamurota, Haruna-machi, Gunma 370-3347, JAPAN
Fax: +81-027-360-8315, e-mail: masa-f@po.iijnet.or.jp, suzuki-t@jty.yuden.co.jp

Defect structures of non-stoichiometric composition $Ba_{1.1}TiO_{3.1}$ epitaxially grown thin film on (100) $SrTiO_3$ substrate by pulsed laser deposition method were studied using transmission electron microscopy (TEM) and X-ray diffraction. Two different type of defect which derived from the non-stoichiometric chemical composition were observed in the film. One was identified as Ruddlesden-Popper-type fault on the (100) plane, identified by high-resolution TEM (HR-TEM) from the [100] direction. The other was twin lamella existing on the (111) plane with nanometer-scale. HR-TEM images and computer image simulation revealed that nanotwins had coherent {111} Σ 3 coincident site lattice (CSL) boundaries with face-shared TiO_6 octahedra. Twin lamellae terminated in the *c*-axis oriented $BaTiO_3$ matrix to form {211} Σ 3 boundaries. In conclusion, excess BaO can be accommodated in Ruddlesden-Popper faults and incoherent (112) Σ 3 interfaces.

Key words: non-stoichiometric composition, $BaTiO_3$, Ruddlesden-Popper-type fault, twin lamella

1. INTRODUCTION

It is well known that non-stoichiometric composition of perovskite compounds leads to formation of defect structures which influence drastically its electrical properties. Therefore, much research has been done on phase reliability, solid solution, defect structures. The defect structure of $BaTiO_3$ was modeled using empirical simulation based on a Born ionic model description of solids[1]. Based on this method, theoretical calculation of defect formation energy of alkaline-earth titanates with excess alkaline-earth oxides has been reported[2], which was suggesting the low solubility of the excess alkaline-earth oxides. The ordering of the crystallographic structure also is introduced by calculating formation energies of Ba_2TiO_4 and Sr_2TiO_4, as a K_2NiF_4 structure based on Ruddlesden-Popper (RP) faults– a composite of perovskite and rock-salt structures – and as a K_2SO_4 structure[4)] with special titanium and oxygen coordination[3]. These results indicated that much less energy was required for the K_2NiF_4 structure Sr_2TiO_4 (-0.11 eV) than for the K_2SO_4 structure Sr_2TiO_4 (0.36 eV), but less energy was required for the K_2SO_4 structure Ba_2TiO_4 (-1.77 eV) than the K_2NiF_4 structure Ba_2TiO_4 (-0.51 eV). The possibility of BaO solubility in $BaTiO_3$ with oxygen and titanium vacancies and the stability of the K_2SO_4 structure Ba_2TiO_4 forming as secondary phase from their larger negative enthalpy were experimentally confirmed. The precipitates of the K_2SO_4 structure Ba_2TiO_4 were observed without any signs of superlattice ordering within $BaTiO_3$ grains in >0.1 mol% excess BaO-$BaTiO_3$ ceramics system using TEM[4]. Thus, there is less possibility to form RP-type BaO intergrowth in BaO-$BaTiO_3$ sintered ceramics system theoretically and experimentally.

In the case of base metal electrode $BaTiO_3$ based ceramics multilayer capacitors as a typical example of practical use with A-site-excess non-stoichiometry, it has to be sintered under a reducing atmosphere to avoid oxidation of base metal electrode (nickel), therefore the $BaTiO_3$ based ceramics has to have a reducing atmosphere-proof characteristic to work as dielectrics. The chemical composition is slightly A-site rich to prevent to form oxygen vacancies playing a part as donor, that is, the excess alkaline earth ions (ex. Ca) and/or rare earth ions derived from the A-site-excess chemical composition occupied B-site of perovskite play as acceptors without formation of RP-type faults. The chemical compositional controlling technique has been established in the ceramics industrial field, however, in the case of perovskite thin film formation it has not been seriously considered before from the practical difficulty of precise chemical compositional control during the processes.

On the other hands, the recent development of instrumentation for epitaxial growth such as molecular beam epitaxy (MBE) and pulsed laser deposition (PLD) has enabled epitaxially grown high-quality $BaTiO_3$ perovskite thin films. The thin film formation process is, however, quite different from that of sintered ceramics, given the much lower processing temperature without thermal equilibrium. Drastic changes of the mechanism for accommodating excess BaO in such a epitaxial grown perovskite thin film is anticipated.

In this paper, we mention the structural analysis of RP-type faults appeared in conventional sintered ceramics, and then report RP-type faults and nanometer scale multiple twin structures in A-site excess $BaTiO_3$ epitaxially grown thin film using high-resolution TEM (HR-TEM) and computer simulation technique.

2. EXPERIMENTAL PROCEDURES

Nonstoichiometric A-site-excess $BaTiO_3$ thin film was fabricated on (100) $SrTiO_3$ substrate by ablating a ceramic target with an ArF eximer laser. The sintered target of $Ba_{1.1}TiO_{3.1}$ was prepared to form a film having the same composition. The $Ba_{1.1}TiO_{3.1}$ target microstructure consists of stoichiometric perovskite $BaTiO_3$ grains including a small amount of Ba_2TiO_4 second phase at grain boundaries. The PLD chamber was equipped with an infrared substrate heating system, in-situ reflection high-energy-electron diffraction (RHEED), and an ArF eximer laser. A $SrTiO_3$ substrate with an atomically smooth (100) surface was prepared by heating at 1000 ℃ for 2 hour after ultrasonic cleaning with acetone and pure water. Deposition was performed in an O_2 ambient (0.1 Pa) and the substrates were heated to 700℃. The thickness of the film is 290nm.

Local micro- and defect structures were evaluated by HR-STEM (Model 002B, Topcon, Tokyo, Japan) equipped with high-resolution CCD (MagaScan, Gatan, Inc., Pleasanton, CA).

3. STRUCTURAL ANALYSIS OF DEFECT STRUCTURES

3.1 High-resolution images of RP-type faults in $SrTiO_3$ Based Ceramics[5]

Figure 1 shows a HR-TEM image of the RP-type faults appeared in $(Sr_{0.85}Ca_{0.15})_mTiO_3$ (m=1.10) by conventional sintering process. The electron beam is parallel to the [100] axis. The arrangement of the black points in the image visually identifies the individual layers of the rock-salt structure between blocks of the perovskite structure as RP-type faults. The inset of Fig. 1 represents a plausible structural model. Next, high

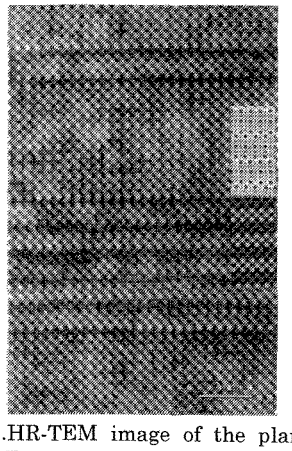

Figure 1.HR-TEM image of the planar faults shown in Fig.4.

resolution simulation , using the multislice method, was achieved under various conditions for Ca-site occupation. For the simulation, two different type of Ca occupation models were proposed: one was a model of 100% of the calcium ions predominantly occupying site of rock-salt structure (model I) and the other was a model of calcium ions randomly occupying sites in both the rock-salt and perovskite structures (model II). HR-TEM images and corresponding simulated images at different defocus settings that verify the validity of image matching are shown in Fig. 2 (Fig. 2 (a) shows a series of HR-TEM images and Figs. 2 (b) and (c) show

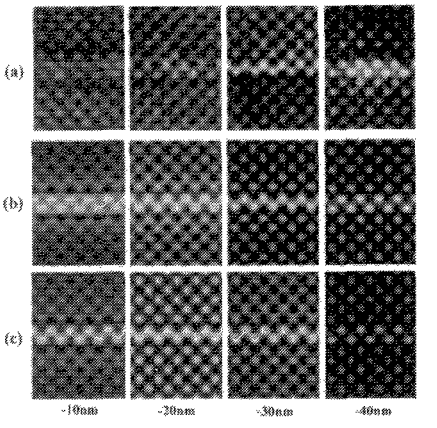

Figure 2.Through-focal series of HR-TEM images, corresponding to the computer-simulation image based on (a) model I(calcium ions predominantly occupy the cation site of the rock-salt structure) and (b and c) model II (calcium ions randomly occupy the cation site in both the rock-salt and perovskite structures). Foil is 5.9 nm thick.

a series of simulated images based on model I and II). The simulated image that is based on model II clearly cannot accurately interpret the high-resolution image, whereas the image that is based on model I can .

The obtained results also are inportant from another reason. The investigated SrO-excess SrTiO3 system is not simple, even though the precise periodicity of the insertion layer of a rock-salt structure between the blocks of perovskite structure can be recognized clearly from the interpreted HR-TEM image that is accompanied by the simulated image. In addition the micro-electron diffraction patterns obtained from faults-free region and faults concentrated region (Fig. 3) suggest a strong periodicity from the $Sr_3Ti_2O_7$-type structure. Thus, the results argue persuasively for adopting the structural model of an SrO-excess $SrTiO_3$ system that is predicted from the shell model, based on calculation of the formation energy of the homologous series of $Sr_{n+1}Ti_nO_{3n+1}$[3]. In other words, the structure of the homologous series can be deduced as blocks of perovskite-structure unit cells of $SrTiO_3$ with randomly accommodated insertion layers of $Sr_3Ti_2O_7$.

Thus, not only RP-type faults and its

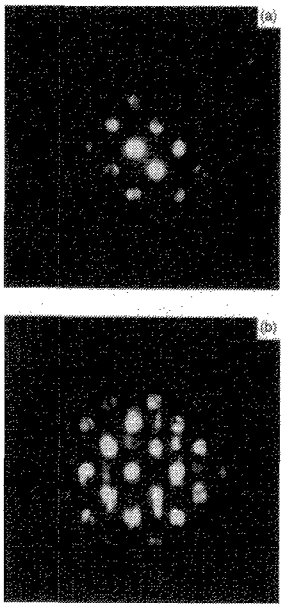

Figure 3. (a)Microdiffraction pattern from defect-free region; (b)Microdiffraction pattern from defect-concentrated region.

structural periodicity, but also the specific ion occupation at the rock-salt structure of cation sites can be clearly identified using HR-TEM image and computer simulation technique.

3.2. RP-type faults in A-site-excess $BaTiO_3$ Epitaxially grown thin film

A cross-sectional HR-TEM image of the A-site-excess $BaTiO_3$ (ABTO) film in the [100] direction (figure 4) shows planar fault-like images along (001) planes in lattice fringes corresponding to the {100} projection of perovskite structure, similar to HR-TEM images reported as RP faults in A-site-excess $SrTiO_3$ ceramics[5], and (Sr, Ca)TiO_3 ceramics[6,7].

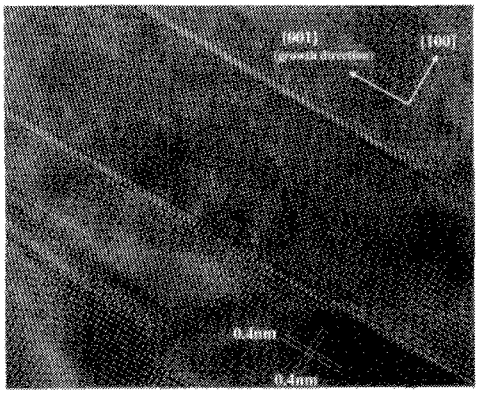

Figure 4. <100> cross-sectional HR-TEM image of A-site-excess $BaTiO_3$ thin film, including(100) planar faults.

HR-TEM atomic structural image of (100) planar faults in <100> projection is shown in Figure 5. Inset is <100>-projected model of RP fault formed perovskite

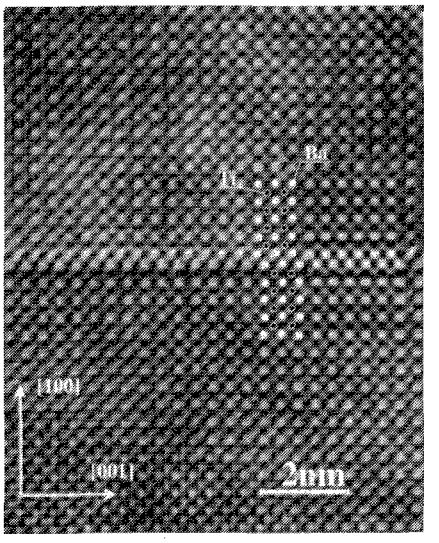

Figure 5. Enlarged image of(100) planar faults in figure 4. Insets are the model and corresponding simulated image. Black and white circles denote titanium and barium ions, and oxygen ions are omitted. The image simulations is multislice-based.

slabs, and corresponding computer-simulated image based on multislice method. Note that HR-TEM image coincide well with computer-simulated image. The (100) planar fault is thus a RP fault, well known as a typical planar fault in SrO-$SrTiO_3$ ceramics, meaning that excess BaO in ABTO thin film can be accommodated by forming RP faults of the BaO-$BaTiO_3$ system.

Note that most of RP faults invariably formed on (100) planes, parallel to the crystal growth direction. RP faults are also not adjacent with a few perovskite slabs, but separated with at least 6 or 7 perovskite slabs, as a result, RP faults do not make an ordered structure represented as $nBaTiO_3$-$Ba_3Ti_2O_7$, expected from experimental results of sintered perovskite ceramics

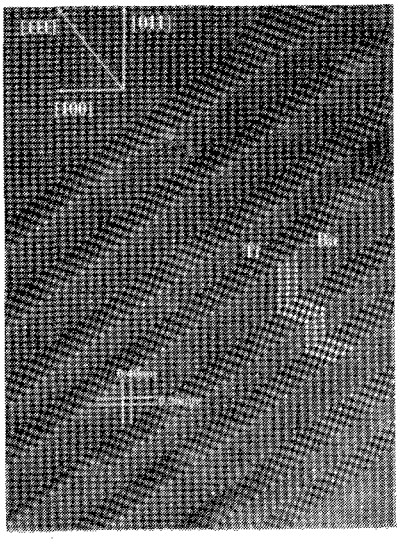

Figure 6. Multiple(111) twin lamellae with cohrent interfaces

cases, such as A-site-excess SrO-$SrTiO_3$ [5] and A-site-excess $(Sr,Ca)TiO_3$ [6,7].

3.3. Nanotwin structures in A-site-excess $BaTiO_3$ Epitaxially grown thin film

The high-resolution TEM image of a twinning area observed in the [101] direction inclined about 45° to the interface is shown in figure 6. Numerous {111} planar faults form nanometer-scale multiple twin lamella structure with coherent {111} twin boundaries, at steps of which some dislocations are found. Lattice fringes near twin boundaries exhibit mirror-symmetrical arrangement, similar to those in $BaTiO_3$ ceramics [8] and in unit cell of hexagonal $BaTiO_3$ [9], but no ordering is seen. This {111} twin boundary is characterized as {111} Σ3 in light of coincident site lattice (CSL) concept. High-resolution TEM images of regions where the lamella are terminated are shown in figures 7 and 8.

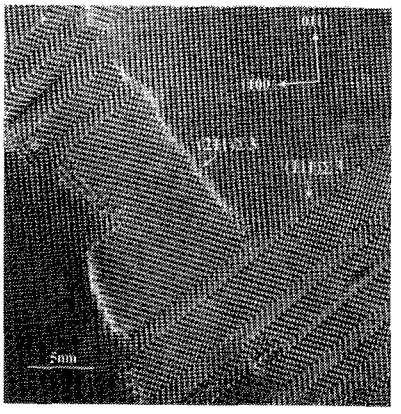

Figure 7. Incoherent{211} Σ 3 boundaries and coherent{111} Σ3 boundaries.

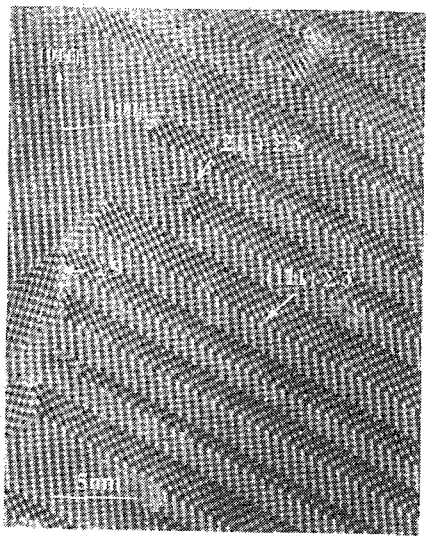

Figure 8. Incoherent Σ9, {211}Σ3, and coherent {111} Σ3 boundaries.

The majority of nanotwin lamellae are completely embedded in the *c*-axis oriented $BaTiO_3$ matrix to form incoherent boundaries other than coherent {111} boundaries, although nanotwin lamellae close to the film surface can penetrate the film. Incoherent twin boundaries of nanotwin lamellae terminating in the matrix is shown in figure 7 at a larger magnification. These boundaries nearly lie on {211} planes and thus can be defined as {211} Σ 3 twin boundaries. On the other hand, Σ 9 twin boundaries generate between nonparallel {111} twin lamellae (figure 8). Figure 9 shows a through-focal series of HRTEM images of a twin boundary in ABTO thin film, corresponding to

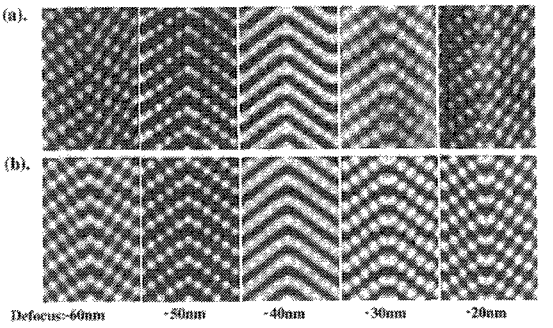

Figure 9. Enlarged image of (100) planar faults in figure 8. Insets are the model and corresponding simulated image. Large and small-white circles denote barium and titanium ions.

computer-simulated images based on the conservative (111) twin model with a mirror BaO_3 plane. Simulated images based on the mirror symmetry model accurately interpret HR-TEM images, suggesting that {111} twins forming in ABTO thin film are conservative. Accordingly, these twins does not seem to function as accommodation sites of excess BaO in ABTO thin film, because they have high-density packing structure at the interface, along which TiO_6 octahedra share faces.

4. DISCUSSION

The existence of RP-type faults is clearly revealed by HR-TEM and its computer simulation image. As far as we know, this type of BaO-$BaTiO_3$ fault is not formed by a conventional sintering with thermodynamic equilibrium, but a low-temperature thin film process with thermodynamic nonequilibrium, such as PLD and MBE, enables the formation of this quasi-stable RP structure. In addition, ordered structure represented as $nBaTiO_3$-$Ba_3Ti_2O_7$, could not be observed, but disordered random faulted planes. This is probably due to uniform supply and limited migration of excess barium ions during crystal growth in the above thin film process. This different behavior of RP fault generation for sintered ceramics and thin film are believed to stem from differences in the thermodynamic equilibrium and thermodynamic nonequilibrium.

The observed {111} nanotwin lamellae terminate in

c-axis oriented epitaxial ABTO thin film to form {211} twin boundaries perpendicular to layered {111} twin boundaries. In contrast to mirror-symmetric coherent {111} twin boundaries, {211} twin boundaries have an asymmetrical structure. The structural characteristic of {211} twins seems attributable to the destruction of a TiO_6 octahedron network and resultant atomic position displacement to obtain highly dense atom packing at the interface. Such a disordered structure acts as accommodation sites for other ions, such as excess barium ions, involving oxygen ions to preserve electrostatic neutral condition. The existence of excess barium ions at incoherent {211} twin boundaries is confirmed by the higher boundary contrast, because, in this projection, columns containing barium and oxygen ions in normal $BaTiO_3$ appear as strong white contrast due to the their comparatively larger scattering potential, substantiated by image simulation. Σ 9 twin boundaries (figure 8) could be synthesized with equivalent four types of twin lamellae, and the possibility of Σ 9 twin boundary appearance is rather lower than that of {211} Σ 3, although more distorted Σ 9 twin boundaries could be more appropriate accommodation sites for excess BaO.

Most RP faults terminate in the $BaTiO_3$ matrix, introducing dislocations with Burgers vectors of type $1/2\boldsymbol{a}$<111>. The formation of RP planar faults thus also contributes to lattice relaxation as to misfit dislocation. On the other hand, the formation of RP faults may prevent the introduction of misfit dislocations from thin film surface, leading to a need for other relaxation mechanisms such as nanotwin formation.

The above consideration suggests that lattice mismatch between $BaTiO_3$ thin film and $SrTiO_3$ substrate is naturally released by introducing misfit dislocations[10] and further the formation of twin lamellae and RP faults. Conversely, the driving force of nanotwin and RP faults formation can be attributed to the nonstoichiometric composition of excess barium ions and to relaxation of misfit strain.

5. SUMMARY

The RP-type faults were formed by the intergrowth of a BaO layer between $BaTiO_3$ perovskite slabs, but no ordered structure represented as $nBaTiO_3$-$Ba_3Ti_2O_7$, as the analogy of A-site-excess SrO-$SrTiO_3$ ceramics was seen. And the formation of nanotwins and RP faults plays a part in accommodating excess BaO, and lattice mismatch relaxation.

References

1) G.V. Lewis and C.R.A. Catlow, *Radiat. Eff.*, **73** 307-14 (1983).
2) K.R. Udayakumar and A.N. Cormack, *J. Phys. Chem. Solids*, **50** 55-60 (1989).
3) K.R. Udayakumar and A.N. Cormack, J. Am. Ceram. Soc., **71** C-469-C-471 (1988).
4) Y.H. Hu, M.P. Harmer and D.M. Smyth, *J.Am. Ceram. Soc.*, **68** 372-76 (1985).
5) M.A. McCoy, R.W. Grimes, and W.E. Lee, *Philos. Mag.*, **75** 833-46 (1997).
6) M. Fujimoto, J. Tanaka, and S. Shirasaki, *Jpn. J. Appl. Phys.*, **27** 1162-66 (1988).
7) M. Fujimoto, T. Suzuki, Y. Nishi, K. Arai and J. Tanaka, *J. Am. Ceram. Soc.*, **81** 33-40 (1998).
8) A Recnik, J. Bruley, W. Mader, D. Kolar and M. Ruhle, , *Phil. Mag.* B, **70**, 1021-1034. (1994).
9) J. W. Nielsen, R.C Linares and S.E Koonce, , *J. Am.. Ceram. Soc.*, **45**, 12. (1962).
10) T. Suzuki, Y. Nishi and M. Fujimoto, *Philos. Mag. A*, in press.

(Received December 11, 1998; accepted February 28, 1999)